ELSEVIER

Journal of Chromatography A, 969 (2002) 273–285

JOURNAL OF CHROMATOGRAPHY A

www.elsevier.com/locate/chroma

Adsorption of poly(methyl methacrylate) and poly(vinyl chloride) blends onto polypyrrole
Study by X-ray photoelectron spectroscopy, time-of-flight static secondary ion mass spectroscopy, and inverse gas chromatography

Marie-Laure Abel[a,1], Mohamed M. Chehimi[a,*], Florence Fricker[a], Michel Delamar[a], Andrew M. Brown[b], John F. Watts[b]

[a]*Interfaces, Traitements, Organisation et Dynamique des Systèmes (ITODYS), Université Paris 7–Denis Diderot, associé au CNRS (UMR 7086), 1 rue Guy de la Brosse, 75005 Paris, France*

[b]*School of Mechanical and Materials Engineering, University of Surrey, Guildford, Surrey GU2 7XH, UK*

Abstract

Poly(vinyl chloride) (PVC) and poly(methyl methacrylate) (PMMA) were co-adsorbed onto conducting, nitrate-doped, polypyrrole ($PPyNO_3$) from tetrahydrofuran and 1,4-dioxane. The surface composition of $PPyNO_3$ before and following polymer adsorption was monitored by X-ray photoelectron spectroscopy and time-of-flight static secondary ion mass spectroscopy which indicated that PMMA and PVC co-adsorb. However, PVC adsorption is substantially higher from 1,4-dioxane, hence a solvent effect. Inverse gas chromatography permitted to determine the dispersive contribution to the surface energy (γ_s^d) and acid–base descriptors of the untreated and polymer blend-coated polypyrrole specimens. Whilst γ_s^d values clearly indicate that the polymer coatings are patchy, acid–base descriptors suggest that the blend patches have a PMMA-rich surface, especially in the case of adsorption from 1,4-dioxane.

Keywords: Adsorption; Inverse gas chromatography; X-ray photoelectron spectroscopy; Mass spectrometry; Poly(methyl methacrylate); Poly(vinyl chloride); Polypyrrole

1. Introduction

Over the past two decades, conducting electroactive polymers such as polypyrrole, polythiophene and polyaniline have been the subject of numerous fundamental and applied research studies [1–5]. These polymers have the unique property to be inherently conducting because the electric current flows via the conjugated polymer chain in contrast with carbon or metal-filled conventional polymers where the electrical current flows via the filler particles. Inherently conducting polymers (ICPs) can be chemically or electrochemically switched from a doped, conducting state to a dedoped, insulating state. They have potent applications in the technologies of composite materials [6,7], electroluminescence [8], biosensors [9] and corrosion control of non-noble metals [10–15]. Particularly, poly-

*Corresponding author. Fax: +33-1-4427-6814.

E-mail addresses: chehimi@paris7.jussieu.fr (M.M. Chehimi), chehimi@paris7.jussieu.fr (M.M. Chehimi).

[1]Present address: School of Mechanical and Materials Engineering, University of Surrey, Guildford Surrey GU2 7XH, UK.

0021-9673/02/$ – see front matter
PII: S0021-9673(02)00894-4

pyrrole (PPy) has attracted much interest because it is easily prepared as films, powders and composites, combines both good thermal and mechanical stability, and maintains its conductivity for several months.

The conductivity of polypyrrole (and other ICPs), however, results in stiff and inflexible polymer chains and the polymer is thus infusible, insoluble in common solvents and otherwise intractable. Polypyrrole is even generally considered to be a cross-linked polymer [16]. Nevertheless, processability can be improved by various methods such as:

(i) co-processing polypyrrole with other flexible insulating polymers [17,18];

(ii) pyrrole polymerisation in untreated and silane-treated porous matrices [19,20];

(iii) chemical synthesis of polypyrrole at the surface of fibres [21–23];

(iv) preparation of colloidal suspensions of polypyrrole microparticles using steric stabilisers [24];

(v) polymerisation of pyrrole in the presence of ultrafine silica sol resulting in raspberry-shaped polypyrrole–silica nanocomposites [25,26];

(vi) polymerization in the presence of polymer colloidal particles resulting in polypyrrole-coated particles [27,28].

As far as composites and coatings are concerned, the long term performance depend critically on the level of interaction and thus adhesion between the matrix and the discontinuous phase (filler or fibre). In the absence of covalent bonds, fundamental adhesion at interfaces is related to the dispersive, polar and acid–base interactions between the substrate and the adsorbate. One of the most used techniques to investigate molecular forces at interfaces is inverse gas chromatography (IGC). We have used IGC to evaluate the London or dispersive contribution to the surface energy (γ_s^d) of polypyrrole powders and acid–base parameters describing their ability to develop hydrogen or Lewis acid–base bonds [29–39]. One important IGC result was the discovery that PPys [37] (and polyaniline [36]) are fairly high surface energy materials, capable of strong interactions either via London dispersion or Lewis acid–base forces. γ_s^d values were in the order of 50–140 mJ/m^2 in the 50–80 °C range, and PPys were ranked as follows: metals > graphite ~ conducting polymers > oxides > carbon fibres > conventional polymers. We have found even much higher γ_s^d values, up to 225 mJ/m^2, for polypyrrole–silica nanocomposites [39], but this was rather partly due to a certain degree of microporosity of such materials. Our results on bulk polypyrrole powders and nanocomposites thus confirm the findings of Vincent et al. [40], using electrophoretic measurements, that Hamaker constants for colloidal polypyrrole particles match those of metals but are significantly much higher than those reported for conventional polymers. Moreover, using reference Lewis acids and bases, we have shown that polypyrrole is an amphoteric polymer which behaves predominantly as a Lewis acid [29,30,33,37,38]. Ageing, degradation and dopant loss resulted in a substantial decrease in γ_s^d values and Lewis acidity of polypyrrole [37].

Bailey and Persand [41] have determined by IGC the surface energy components of vapour deposited PPyCl on the inner wall of a capillary column. The authors obtained high γ_s^d values (144 mJ/m^2 + 0.2965T mJ/m^2/K) in the 40–60 °C and strong acid–base interactions with specific probes such as THF, ethylacetate and acetonitrile, thus confirming the trends of our results [37]. Surprisingly, in determining acid–base constants using the linear solvation energy relationship (LSER), the authors obtained a negative value for the acidic character of polypyrrole but a fairly strong basic character. Whilst the latter result is understandable due to the amphoteric character of polypyrrole, a negative value for the acidity constant is in total contrast with the values of the specific interaction energies obtained by the authors on the one hand, and do not reflect the structure of polypyrrole, on the other hand. Indeed, polypyrrole should be acidic in nature due to the N–H bond in pyrrole units and the positive charge of the polymer backbone.

Since London dispersive and Lewis acid–base interactions are relevant to adsorption, wetting and adhesion of polymers [42,43], we extended our investigations on ICP surface properties to the study of adsorption of flexible polymers onto the stiff polypyrrole (which can act as a conducting filler). We have selected poly(methyl methacrylate), PMMA, a conventional flexible insulating homopolymer which is often used as a model polymer in adhesion and wetting reports [42–46]. We used X-ray photoelectron spectroscopy (XPS) and time-of-flight static

secondary ion mass spectroscopy (TOF-SSIMS) to evaluate the surface composition of PMMA-coated PPys and determine adsorption isotherms, which usually fitted the Langmuir model [47–49]. We have shown that the nature of the casting solvent is crucial to the extent of PMMA adsorption [47,50]. IGC was further used to study the solvent effect on the dispersive and acid–base properties of PMMA-coated, chloride-doped polypyrrole (PPyCl) [38]. It was concluded that good, acidic solvents lead to inhomogeneous coatings whereas poor, neutral or basic solvents lead to the formation of homogeneous coatings. An AFM study of PMMA films solvent-cast onto para-toluene sulfonate-doped polypyrrole (PPyTS) surfaces corroborated the IGC findings on the coated polypyrrole powder [51].

The aim of this work is to characterize the surface energy of $PPyNO_3$ by IGC at infinite dilution before and following adsorption of poly(vinyl chloride), PVC, and PMMA from binary mixtures in either tetrahydrofuran (THF) or 1,4-dioxane (DXN) (see polymer structures in Fig. 1). XPS and TOF-SSIMS provided a survey of the change in the surface chemical composition of $PPyNO_3$ powder induced by the various flexible polymer coatings.

We have chosen PVC and PMMA, two model polymers of which acid–base properties are well documented [44,45]. The former is predominantly acidic and the latter fairly basic. It was previously shown by dynamic mechanical measurements and optical clarity that PMMA and PVC yield miscible blends [52]. However, it was reported that PVC–PMMA blend surface was PMMA-rich if the blend was cast from THF but not from methylacetate [53]. Further evidence for phase separation at the surface of this system has been given by imaging XPS [54] and TOF-SSIMS studies [55,56]. The rationale for combining IGC with XPS and TOF-SSIMS is that the three techniques are complementary: XPS and TOF-SSIMS probe 10 and 2 nm, respectively, whereas IGC is sensitive to the outermost adlayers of stiff materials such as polypyrrole and flexible polymers below their T_g values, glass transition temperature (this is the case of PMMA and PVC in this work).

2. Experimental

2.1. Synthesis of polypyrrole

Doubly-distilled pyrrole (Aldrich, Steinheim, Germany; 1.75 ml, 0.025 mol) was added to ≈100 ml of a stirred aqueous solution of $Fe(NO_3)_3 \cdot 9H_2O$ (Prolabo, Fontenay Sous Bois, France; 30.3 g, 0.075 mol) and 1.5 g (0.025 mol) of urea (Fluka, Buchs, Switzerland). The solution was stirred for 2 h at 0 °C under a stream of nitrogen. The $PPyNO_3$ powder was then collected in a Büchner funnel flask and thoroughly rinsed with distilled water until the washings were clear. The $PPyNO_3$ powder was then dried in a vacuum desiccator for at least 24 h. The powder was sieved to ≈100 μm before surface characterization and polymer adsorption experiments.

2.2. PMMA and PVC adsorption

We used a 100-ml volumetric flask containing the solution of PMMA (Aldrich, Steinheim, Germany; M_r 101 000) and PVC (Janssen, Geel, Belgium; M_r 180 000) mixtures in THF (Aldrich, Steinheim, Germany) or 1,4-dioxane (Janssen, Geel, Belgium). PMMA initial concentration was varied (0.88, 1.56 and 2.64 g/l) that of PVC kept constant (0.88 g/l). The solvents were slightly warmed to achieve a

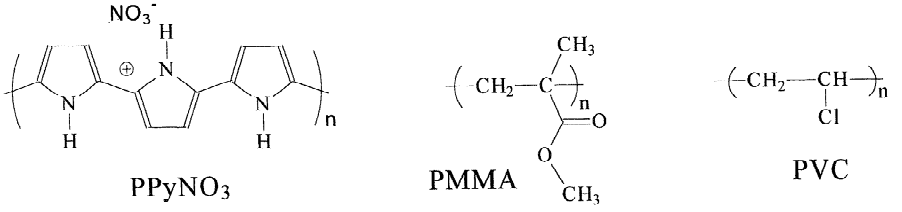

Fig. 1. Structure of $PPyNO_3$, PMMA and PVC.

complete dissolution of PMMA. This was not necessary for PVC because it was readily dissolved in either THF or 1,4-dioxane. After the solution was equilibrated at ambient temperature, 250 mg of $PPyNO_3$ powder were introduced into the volumetric flask and the suspension stirred for 1 h. The suspension was filtered and vacuum-dried overnight before IGC, XPS and TOF-SSIMS characterisations. $PPyNO_3$ specimens coated with a blend of PMMA and PVC are designated PPy–PMMA–PVC.

2.3. X-ray photoelectron spectroscopy (XPS)

XPS signals were recorded using a VG Scientific Escalab MKI system (East Grinstead, UK) operated in the constant analyser energy mode. An Al Kα X-ray source (1486.6 eV) was used at a power of 200 W and the pass energy was set at 50 eV. The stability of PVC under the X-ray gun has systematically been checked by monitoring the Cl2p signal at the beginning and the end of each analysis. There was no evidence for such a degradation of PVC within the the time scale of the XPS analyses.

Digital acquisition was achieved with a Cybernetix system (Marseille-Luminy, France) and the data collected with a personal computer. Data processing was achieved with laboratory-written software. The surface composition (in atom%) of the various samples was determined by considering the integrated peak areas of C1s, N1s, O1s and Cl2p, and their respective experimental sensitivity factors. The surface composition as %*A*, the fractional concentration of a particular element *A* was computed using:

$$\%A = (I_A/s_A)/\sum(I_n/s_n)\cdot 100\% \quad (1)$$

where I_n and s_n are the integrated peak areas and the sensitivity factors, respectively.

2.4. TOF-SSIMS

The TOF-SSIMS spectra were acquired using a VG Scientific Type 23 system (Fisons Instruments, East Grinstead, UK) equipped with a double stage reflectron time-of-flight analyser and a MIG300PB pulsed liquid metal ion source. Static SIMS conditions (i.e. a total ion dose of less than 1.10^{12} ions/cm^2 during analysis) were employed using a pulsed (20 kHz and 20 ns) 30 keV $^{69}Ga^+$ primary ion beam rastered at TV rate of over an area of 0.9×0.9 mm. Specimens were prepared by pressing the powders on double sided tape against aluminium foil to avoid any contamination. The spectra were acquired over a mass range of m/z 5–400 in both the positive and the negative ion modes. However, useful information could be gained from the positive ion mode only, a situation we faced before [57].

2.5. IGC

A gas chromatograph, Girdel 330 (Giravions Dorand, Suresnes, France), fitted with a flame ionization detector was used. The carrier gas was a high purity grade nitrogen (Fluka, Buchs, Switzerland), the flow-rate of which was set at 20 ml/min. The injector and detector temperatures were set at 110 °C. Stainless steel columns (Varian, Les Ulis, France) were 20–30 cm×1/8th in O.D. (1 in=2.54 cm). They were packed with 60–200 mg of uncoated and coated polypyrrole powders. PMMA 5.6% (w/w) was coated onto Chromosorb (Celite, Lompoc, CA, USA) from chloroform (Aldrich, Steinheim, Germany) and PVC from THF onto Aeropak (Walnut Creek, CA, USA) at at mass loading of 5% (w/w) and according to the soaking method of Al-Saigh and Munk [58]. Quarter inch O.D. PTFE columns were packed with ≈10 g of supported PMMA and PVC, and were used as control columns. All stationary phases were conditioned at 48 °C for 15 h. Probes were injected manually in triplicate by a gas tight Hamilton syringe (Bonaduz, Switzerland). The syringe was purged as many times as necessary in order to reach the detection limit of the apparatus. The signals were recorded with a Delsi 21 digital recorder (Delsi Instruments, Suresnes, France) and the retention times were calculated graphically [59]. The probes were high purity grade *n*-alkanes, chloroform and THF. The properties of the probes are reported in Table 1, where *DN* [60] and *AN** [61] are the Gutmann's donor and acceptor numbers. *AN** values are those corrected for van der Waal's interactions and converted from ppm units into kJ/mol [61].

The retention times (t_R) were corrected for the gas

Table 1
Probes used to characterise the various materials

Probes	Abbreviation	b.p. (°C)	*DN*	*AN**	*DN*/*AN**	Supplier
n-Pentane	C_5	36.1				Prolabo
n-Hexane	C_6	68.7				Prolabo
n-Heptane	C_7	98.4				Prolabo
n-Octane	C_8	125.7				Fluka
n-Nonane	C_9	150.8				Fluka
n-Decane	C_{10}	174.1				Fluka
Chloroform	$CHCl_3$	61.2	0	22.6	0	Aldrich
Tetrahydrofuran	THF	66.0	83.7	2.1	39.9	Prolabo

DN and *AN** are in kJ/mol. See text for suppliers.

holdup, t_0, of the column using methane (Air Liquide) as a non-interacting marker.

At infinite dilution (zero coverage), ΔG_a, the free energy of adsorption, is related to V_N, the net retention volume, by:

$$-\Delta G_a\,(\text{in kJ/mol}) = RT\,\ln(V_N) + C \qquad (2)$$

where R is the gas constant, T is the column temperature and C is a constant which takes into account the weight and specific surface area of the packing material and the standard states of the probes in the mobile and the adsorbed states [62].

3. Results and discussion

3.1. X-ray photoelectron spectroscopy (XPS)

Fig. 2 shows the XPS survey scan of $PPyNO_3$ before and after adsorption of a PVC and PMMA blends. Fig. 2b exhibits a significantly intense Cl2p peak accounting for the adsorption of PVC and, simultaneously, a relative attenuation of the N1s peak from the $PPyNO_3$ substrate. The O1s peak remains intense due to the co-adsorption of PMMA. Polypyrrole is thus a sorbent for PVC of which acidic sites of PVC (C–H in ClCH) probably interact with the basic sites of the former (dopant, C=C double bonds). Conversely, the ester group from the PMMA repeat units interact specifically with the acidic sites of polypyrrole (σ^* anti-bonding orbital located on the N–H bond, and the positively charged backbone).

Fig. 3 depicts the N1s peak from the $PPyNO_3$ substrate. The first complex peak centred at ≈400 eV is due to the pyrrole repeat units whereas the second is due to the nitrate dopant. Only the first complex peak due to the PPy backbone will be used in the calculation of the relative proportions of $PPyNO_3$, PVC and PMMA. These can be estimated using the contribution of each polymer to the total C1s intensity signal. Given the number of carbon atoms (n_C) per repeat unit for each polymer (2, 4 and 5 for PVC, $PPyNO_3$ and PMMA, respectively), the relative proportion of each polymer was calculated by:

$$\%\ \text{polymer} = \frac{\dfrac{\text{C1s(polymer)}}{n_C}}{\dfrac{\text{C1s(PPyNO}_3\text{)}}{4} + \dfrac{\text{C1s(PMMA)}}{5} + \dfrac{\text{C1s(PVC)}}{2}} \cdot 100\% \qquad (3)$$

where C1s(polymer) is the the contribution of a given polymer to the total C1s peak area. This equation takes into account the stoichiometric formula of each polymer: $C_4N(NO_3)_{0.3}$, C_5O_2 and C_2Cl for $PPyNO_3$, PMMA and PVC, respectively (hydrogen is excluded because it is not detected by XPS). The contribution of each polymer to C1s peak area was assessed using the independent XPS analyses of each of the three polymers. For PVC and $PPyNO_3$, we have determined C1s/Cl2p and C1s/N1s intensity ratios, respectively. It follows, by subtraction, that:

$$C_{1s}(\text{PMMA}) = C_{1s}(\text{total}) - C_{1s}(\text{PVC}) - C_{1s}(\text{PPyNO}_3) \qquad (4)$$

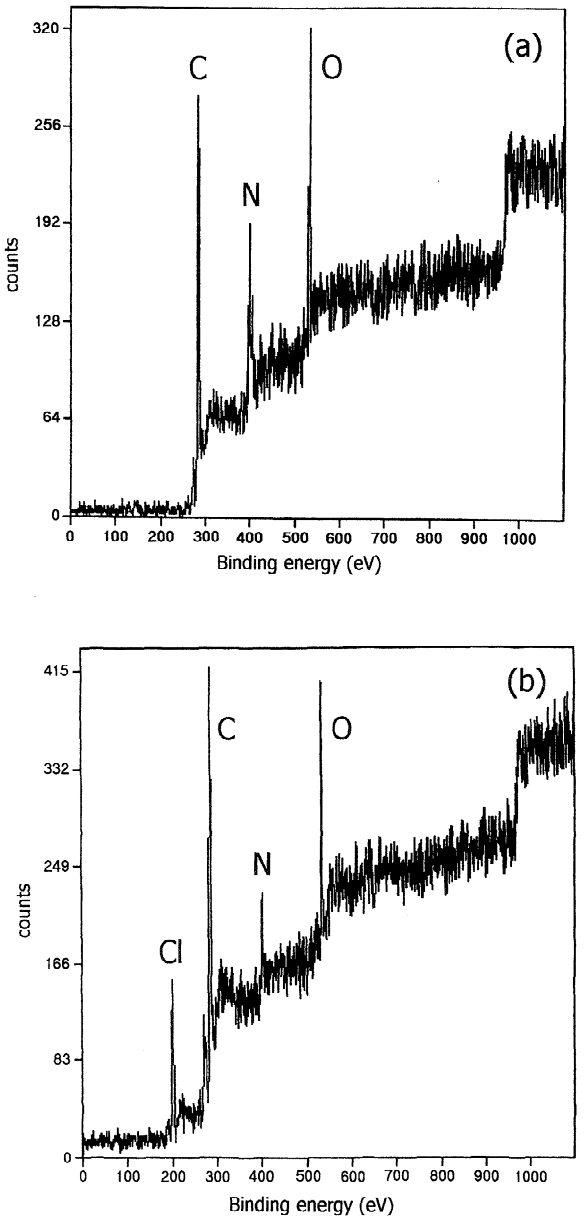

Fig. 2. XPS survey scans of (a) uncoated, and (b) PMMA–PVC blend-coated $PPyNO_3$. PMMA and PVC initial concentrations were 0.88 g/l.

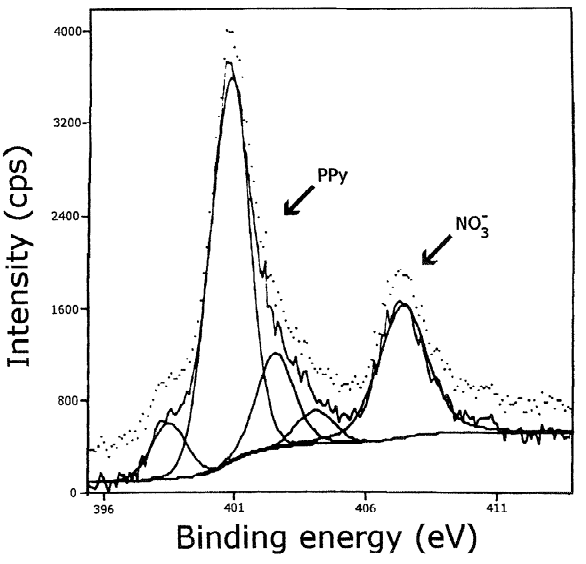

Fig. 3. Structure of the N1s XP spectrum from $PPyNO_3$. The complex peak centred at 400 eV is due to PPy backbone and the one at 407 eV is due to the NO_3^- dopant. The PPy signal was peak-fitted with four components assigned (by increasing binding energy) to imine defects, N–H bonds, and two types of positively charged nitrogen atoms.

where C_{1s}(total) is the integrated C1s peak area recorded for a coated polypyrrole powder.

Fig. 4 displays the relative proportions of polymer repeat units versus the initial concentration of PMMA. The solvent nature is an important parameter since PVC adsorption is three to six times higher in DXN than in THF. Adsorption of PMMA is roughly the same from the two solvents. Since THF is more basic than DXN (Gutmann's *DN* equal 83.8 and 61.9 kJ/mol, respectively) it should interact much more strongly with $PPyNO_3$. Indeed, it was shown by IGC at infinite dilution that the acid–base contribution to free energy of adsorption (ΔG_a^{AB}) of THF and DXN onto polypyrrole powders is in the range of 3.4–10.1 and 2.9–5.0 kJ/mol, respectively [37]. THF is thus a stronger competing solvent than dioxane, especially in the case of PVC.

The thickness (d) of the polymer blend overlayers was determined from the attenuation of the N1s peak intensity of the polypyrrole backbone (nitrate dopant excluded):

$$d = \lambda_{N1s} \sin\theta \ln\left(\frac{I_{N1s}^{\infty}}{I_{N1s}}\right) \quad (5)$$

where θ the photoelectron take-off angle relative to the surface, I_{N1s}^{∞} the N1s intensity from the untreated polypyrrole and I_{N1s}, the N1s intensity peak from

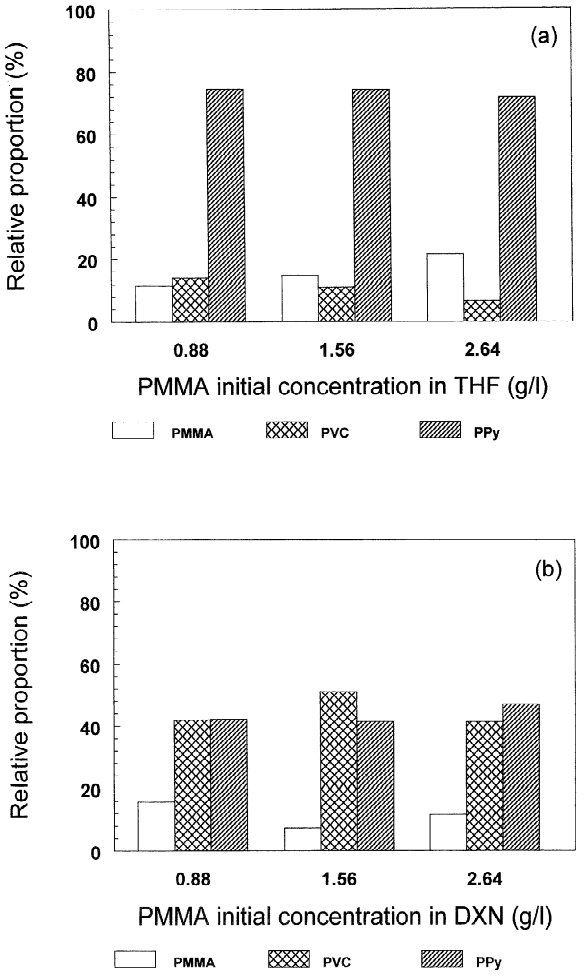

Fig. 4. Relative proportions of $PPyNO_3$, PMMA and PVC determined by XPS versus the initial concentration of PMMA in THF and dioxane.

blend-coated polypyrrole. Assuming a spherical shape of polypyrrole elemental particle, the average value of $\sin\theta = \frac{1}{2}$ [63].

Table 2 reports the thickness of the various coatings at indicated initial conditions. The average thickness (assuming a continuous blend overlayer at the surface of the particles) obtained in DXN is 1.5 time larger than that obtained in THF. The low values corresponding to THF suggest patchy coatings as a monolayer of PVC or PMMA is ≈4–5 Å thick [64]. The values reported for the polymer blend adsorption from DXN are higher than PVC or PMMA monolayer thickness. IGC will readily indicate whether these coatings are patchy or not as the derived thermodynamics data will reflect the nature of either the substrate or the adsorbates (see below).

Table 2
Surface composition by XPS of $PPyNO_3$ coated with PMMA and PVC

Solvent	[PMMA] (g/l)	Thickness (Å)
THF	0.88	3.7
	1.56	2.7
	2.64	3
Dioxane	0.88	8.6
	1.56	9.7
	2.64	9.1

PVC initial concentration was 0.88 g/l for the six systems.

3.2. TOF-SSIMS

Fig. 5 shows TOF-SSIMS spectra of $PPyNO_3$ in the m/z range of 20–40 a.m.u before and following polymer blend adsorption. PVC is easily detected by

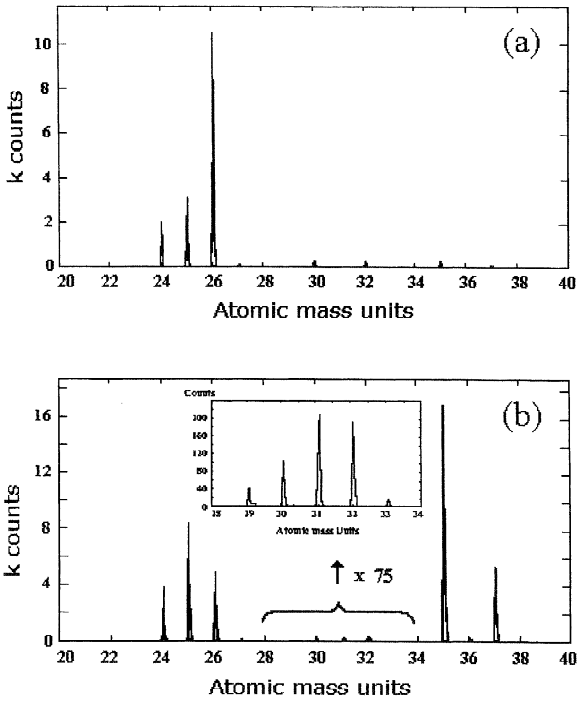

Fig. 5. TOF-SSIMS spectra of (a) uncoated, and (b) PMMA–PVC blend-coated $PPyNO_3$. PMMA and PVC initial concentrations were 2.64 and 0.88 g/l, respectively. The insert in (b) shows a mass peak centred at 31 and due to OCH_3^- from PMMA.

its very intense peak doublet at m/z 35 and 37 from the chlorine isotopes $^{35}Cl^-$ and $^{37}Cl^-$. Enlargement of the 28–34 m/z region in Fig. 5b shows a characteristic OCH_3^- peak at 31 a.m.u from PMMA. This clearly shows that PMMA has effectively been adsorbed, an information which was not straightforward from XPS.

The surface composition of the blend-coated polypyrrole was determined using the diagnostic fragments reported in Table 3. For PVC we used the elemental ion $^{37}Cl^-$, the minor isotope, in preference to the more intense $^{35}Cl^-$ ion because its intensity was comparable to that of the $^{26}CN^-$ ion. The TOF-SSIMS relative proportions of adsorbed PMMA and PVC were evaluated using the following respective ratios (in %):

$$K_{31} = I_{31}/(I_{31} + I_{26} + I_{37}) \cdot 100\% \quad (6a)$$

and

$$K_{37} = I_{37}/(I_{31} + I_{26} + I_{37}) \cdot 100\% \quad (6b)$$

where I_{26}, I_{31} and I_{37} are the integrated signals of the mass peaks centred at 26, 31 and 37 Daltons.

Adsorption of PMMA and PVC (expressed by K_{31} and K_{37}, respectively), depicted in Fig. 6, increases approximately by a factor of 2 and 1.5, respectively, on going from THF to DXN. This rather contrasts with XPS results which indicate that PMMA adsorption (%PMMA) from THF is comparable to that from dioxane, and PVC adsorption (%PVC) is three to six times larger from the latter solvent. Therefore, PMMA is most likely depleted towards the outermost coating overlayer. TOF-SSIMS results differ from those derived from XPS data due to the difference in the sampling depths, the former having a superior surface specificity. The hypothesis of PMMA depletion (especially in the case of DXN) can be checked further via IGC.

Table 3
Diagnostic fragments used in TOF-SSIMS for the characterization of $PPyNO_3$, PMMA and PVC

Polymer	Fragment	m/z
$PPyNO_3$	CN^-	26^-
PMMA	OCH_3^-	31^-
PVC	Cl^-	37^-

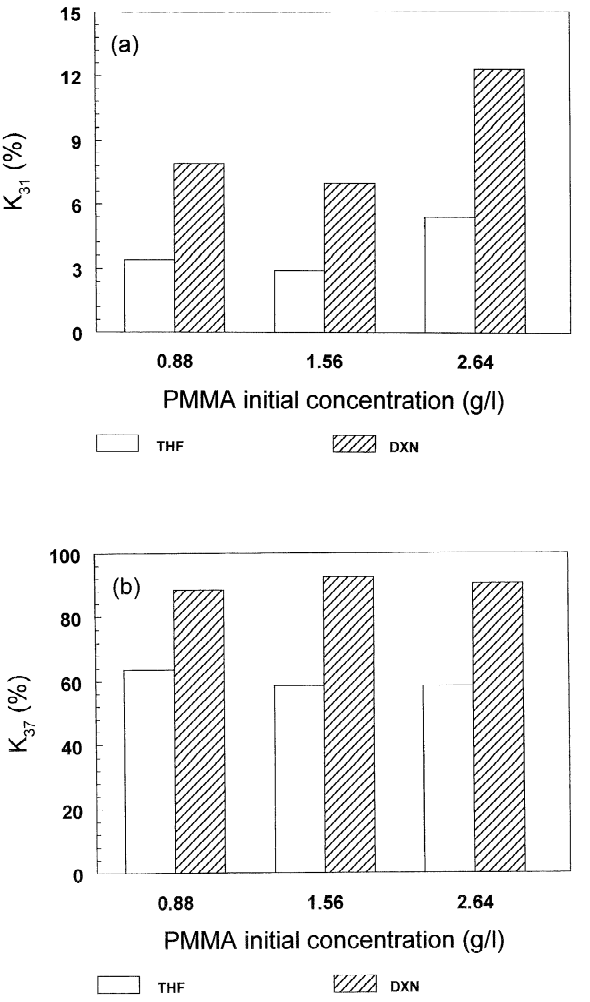

Fig. 6. TOF-SSIMS determination of PMMA (K_{31}) and PVC (K_{37}) adsorption from THF and DXN versus the initial concentration of PMMA (see Eqs. (6a) and (6b) for the definition of K_{31} and K_{37}).

3.3. IGC

n-Alkanes (apolar solutes), THF (reference Lewis base) and chloroform (reference Lewis acid) were used to tag the dispersive, acidic and basic properties of the coated polypyrrole powders, respectively. In Fig. 7, $RT \ln V_N$ is plotted vs. the number of carbon atoms in the *n*-alkane series injected in columns packed with untreated $PPyNO_3$, PVC–PMMA blend-coated $PPyNO_3$ and PMMA coated onto Chromosorb. Excellent linear correlations are generated for

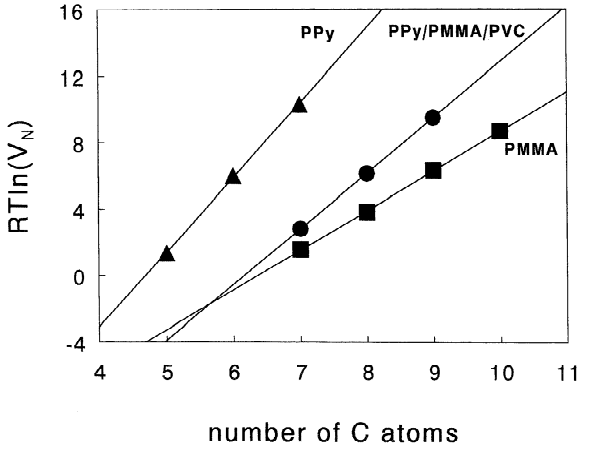

Fig. 7. $RT\ln(V_N)$ vs. the number of carbon atoms in the *n*-alkane series adsorbed on $PPyNO_3$, a PPy–PMMA–PVC and PMMA at 48 °C.

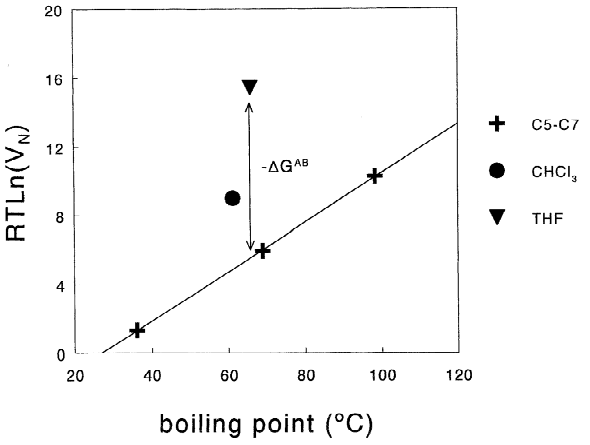

Fig. 8. $RT\ln(V_N)$ vs. the boiling point for probes adsorbed onto a PPy–PMMA–PVC.

the three materials. The steepest slope (a measure of $\Delta G_a^{CH_2}$, the free energy of adsorption per methylene group [65]) is obtained for $PPyNO_3$, a qualitative indication that it has the most energetic surface. γ_s^d is related to $\Delta G_a^{CH_2}$ by:

$$\gamma_s^d\ (\mathrm{mJ/m^2}) = \frac{1}{4\gamma_{CH_2}} \cdot \left[\frac{\Delta G_a^{CH_2}}{N.a_{CH_2}} \right]^2 \quad (7)$$

where N is the Avogadro number and a_{CH_2} is the cross-sectional area of an adsorbed CH_2 group (6 $Å^2$). γ_{CH_2} is the surface free energy of a solid containing only methylene groups such as polyethylene, and is expressed by [65]:

$$\gamma_{CH_2}\ (\mathrm{in\ mJ/m^2}) = 36.8 - 0.058T\ (°C) \quad (8)$$

Fig. 8 illustrates the assessment of ΔG_a^{AB} by the approach of Brookman and Sawyer [66]: $RT\ln V_N$ values are plotted vs. the boiling points (b.p.) of the various probes for one of the polymer blend-coated polypyrrole samples. An excellent linear plot is generated with *n*-alkanes, whereas the markers corresponding to chloroform and THF significantly deviate from the linear plot, an indication of specific acid–base interactions between the probes and the adsorbent. For these probes, the vertical distance from the reference line yields:

$$-\Delta G_a^{AB}\ (\mathrm{in\ kJ/mol}) = RT\ln(V_N/V_{N,ref}) \quad (9)$$

where $V_{N,ref}$ is the net retention volume of a hypothetical *n*-alkane that boils at the same temperature as the test acidic or basic probe.

Acid–base constants K_A and K_D were calculated using:

$$-\Delta G_a^{AB}\ (\mathrm{in\ kJ/mol}) = K_A \cdot DN + K_D \cdot AN^* \quad (10)$$

where DN and AN^* are the donor and acceptor numbers of the reference solutes. Eq. (10) is based on the approach of Saint Flour and Papirer [67] but simply relates ΔG_a^{AB}, and not ΔH_a^{AB} (the heat of acid–base adduct formation) to Gutmann's numbers.

Table 4 reports the values of γ_s^d, K_D, K_A and K_D/K_A ratio (a measure of the overall basicity) for the various blend-coated $PPyNO_3$ powders, $PPyNO_3$, PVC and PMMA.

Fig. 9 depicts a plot of γ_s^d vs. the relative proportion of polypyrrole determined by XPS: γ_s^d roughly decreases for increasing sum of the relative proportions of PMMA and PVC (decreasing relative proportion of PPy). DXN yields lower γ_s^d values since it permits to adsorb more insulating conventional polymers. The intermediate values of γ_s^d for the coated $PPyNO_3$ indicate that adsorption of all PVC and PMMA blends results in patchy coatings. In addition, γ_s^d values suggest that the surface coverage of polypyrrole is lower in THF since more high-energy sites are probed by the *n*-alkanes. This contrasts with our previous findings on PMMA-

Table 4
Dispersive and acid–base properties of polymer blend-coated polypyrrole and reference materials

Materials	$[PMMA]_i$ (g/l)	γ_s^d	$K_D \times 100$	$K_A \times 100$	K_D/K_A
$PPyNO_3$		113	19.2	11.5	1.7
PVC		31	21.8	14.9	1.5
PMMA		40	35.4	7.6	4.7
$PPyNO_3$–PVC–PMMA–THF	0.88	54.7	24.4	10.2	2.4
	1.56	60.8	29.2	11.5	2.5
	2.64	63	26.9	10.6	2.5
$PPyNO_3$–PVC–PMMA–Dioxane	0.88	48.7	26	10.1	2.6
	1.56	55	26.5	10.1	2.6
	2.64	54	24.5	10.6	2.3

PVC initial concentration = 0.88 g/l.

coated PPyCl prepared in DXN [38] of which γ_s^d value was 39.2 mJ/m^2 for a relative proportion of PMMA of 11.4%. In the present work, even for the sample with 15.8% PMMA, γ_s^d value is 48.7 mJ/m^2. It is also interesting to note that for a lower initial concentration of polymer in THF, all γ_s^d values are comparable or lower than the value of 69.4 mJ/m^2 found for PMMA-coated polypyrrole using an initial PMMA concentration of 7.5 g/l. This minimization of the surface energy of polypyrrole is due to the larger amount of adsorbed polymer obtained in the present work by comparison to the single polymer system studied previously [38].

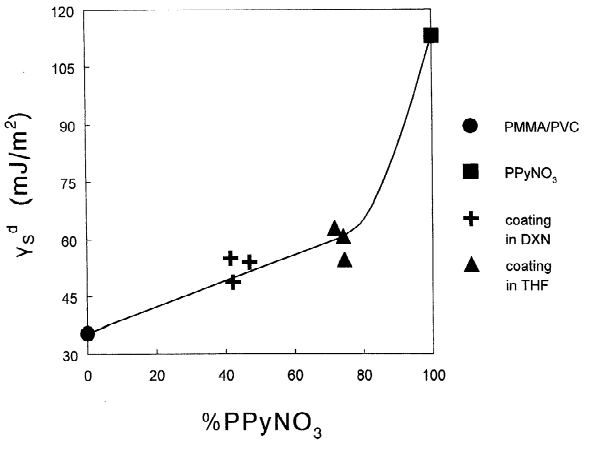

Fig. 9. γ_s^d values versus the relative proportion of $PPyNO_3$ (determined by XPS) for (●) PMMA and PVC, (+) $PPyNO_3$ after coating in DXN, (▲) $PPyNO_3$ after coating in THF, and (■) uncoated $PPyNO_3$. In the case of PVC and PMMA reference materials, an average value (35.5 m/m^2) of the corresponding γ_s^d values was chosen for the plot.

The donor and acceptor constants determined via IGC decrease in the following order:

K_D: PMMA > coated $PPyNO_3$ > PVC > $PPyNO_3$

K_A: PVC > $PPyNO_3$ > coated $PPyNO_3$ > PMMA

K_D/K_A: PMMA > coated $PPyNO_3$ > $PPyNO_3$ ~PVC

Given that the polymer blend overlayers are patchy as judged from γ_s^d values, the trends of acid–base constants suggest that the patches surfaces are PMMA-rich. Indeed, if the surface of the patches was PVC-rich, K_D and the overall basicity K_D/K_A would match those of PVC and $PPyNO_3$. We have shown elsewhere [38] that for a homogeneous PMMA overlayer, the dispersive and acid–base properties of coated PPyCl match those of the adsorbate. At 48 °C, the molecular probes interact with the outermost layers sites since $PPyNO_3$ is a rigid polymer and PVC and PMMA are below their T_g values (80 and 105 °C, respectively). Therefore, adsorption phenomena of the molecular probes only occur [59]. Given this, we propose to assess the surface composition in polymers using γ_s^d, K_D and K_A data for the coated polypyrrole powders and the reference uncoated polypyrrole, PVC and PMMA characterized independently. However, the following assumptions must be considered:

(i) γ_s^d, K_D and K_A for the polymer blend-coated polypyrrole is a weighed average value of these data determined for the three polymers taken separately. This is based on the functional group contributions to the surface energy of a given polymer [68]. It is thus assumed that this is true for a heterogeneous surface and that the total surface energy is a weighted value of the contributions of all functional groups present

at the surface of polymer blend-coated polypyrrole (regardless to which polymer they belong).

(ii) The molecular probes do not adsorb preferentially onto the high energy sites of polypyrrole if they are uncoated.

Given this, the surface relative proportions of polypyrrole, PMMA and PVC can be estimated from the following equation system:

$$\begin{pmatrix} \gamma_s^d \\ K_D \\ K_A \end{pmatrix}_{\text{blend}-\text{PPy}} = \begin{pmatrix} \gamma_s^d(\text{PPy}) & \gamma_s^d(\text{PMMA}) & \gamma_s^d(\text{PVC}) \\ K_D(\text{PPy}) & K_D(\text{PMMA}) & K_D(\text{PVC}) \\ K_A(\text{PPy}) & K_A(\text{PMMA}) & K_A(\text{PVC}) \end{pmatrix} \times \begin{pmatrix} x \\ y \\ z \end{pmatrix} \quad (11)$$

where x, y and z are the relative proportions of $PPyNO_3$, PMMA and PVC, respectively. The computed values (in%) of x, y and z are reported in Table 5. It is worth to note that for both solvents, the relative proportion of $PPyNO_3$ determined by IGC (27.7–34.1% in DXN and 19–26.5% in THF) is lower than that determined via XPS (42.2–47% in DXN and 71.7–74.5% in THF). This is due to the fact that the former technique probes the outermost layers whereas the analysis depth of the latter is 5–10 nm. IGC is thus more sensitive to the adsorbates whereas XPS probes the buried surfaces where polypyrrole substrate is more abundant.

Fig. 10 depicts a plot of the relative proportion of PMMA (Fig. 10a) and PVC (Fig. 10b) determined by IGC versus those determined by XPS for the blend-coated polypyrrole powders. A reference line of slope 1 and intercept zero is drawn for the hypothetical case where the relative proportions determined by both techniques match. When a marker is plotted above the reference line, it means that the corresponding polymer is more detected by IGC than by XPS. In other words, for given conditions, the polymer is segregated to the free surface of the coated polypyrrole.

Table 5
IGC estimation of the relative proportions of $PPyNO_3$, PMMA and PVC at the surface of polymer blend-coated $PPyNO_3$

$[PMMA]_i$ (g/l)	IGC		
	$PPyNO_3$	PMMA	PVC
1,4-Dioxane			
0.88	27.7	36.3	28.5
1.56	28.3	48.2	30.7
2.64	34.1	43.6	22.6
THF			
0.88	19	44.4	30.5
1.56	25.7	45.8	24.6
2.64	26.5	34.4	33.1

Initial concentration of PVC = 0.88 g/l.

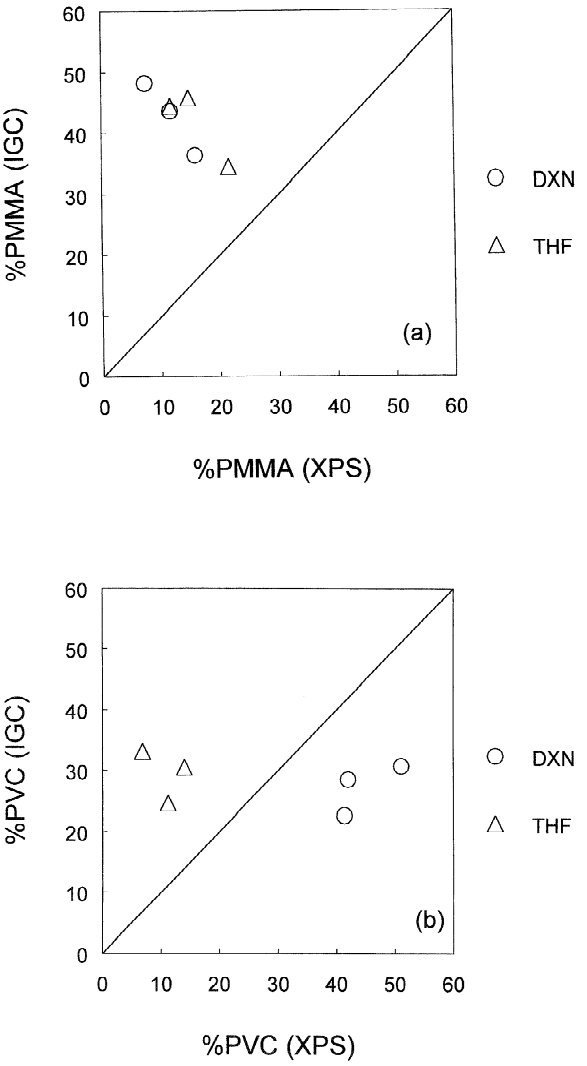

Fig. 10. Relationship between the relative proportions of (a) PMMA, and (b) PVC estimated by IGC versus those estimated by XPS (see Eq. (11) for IGC and Eqs. (3) and (4) for XPS).

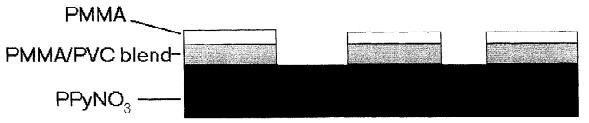

Fig. 11. Illustration of a polypyrrole surface partially coated with a PMMA–PVC blend.

Fig. 10a indicates that in both solvents %PMMA determined by IGC is invariably higher than that assessed by XPS. In contrast, %PVC decreases in the order IGC>XPS for THF and not dioxane. This result can be interpreted as follows: from dioxane, the total amount of adsorbed PVC and PMMA is high enough to initiate the formation of multilayered patches with PVC segregating to the polypyrrole–blend interface and PMMA to the blend–air interface as illustrated in Fig. 11.

The IGC approach provides very surface-specific information about PMMA segregation that parallel the TOF-SSIMS results presented above. Our findings are also in line with the TOF-SSIMS study of PVC–PMMA blend surface reported by Briggs et al. [56].

4. Conclusion

This paper reports a study of adsorption of PVC and PMMA blends onto conducting $PPyNO_3$ powder from THF and 1,4-dioxane, by means of XPS, TOF-SSIMS and IGC. The surface compositions of the various PVC–PMMA blend-coated polypyrrole powders were determined by XPS and TOF-SSIMS, whereas their dispersive and acid–base properties were assessed by IGC. The main results we have reached in this study are the following:

(1) Polypyrrole simultaneously adsorbs PVC and PMMA at an extent that depends on the initial polymer concentrations and more importantly the solvent nature, 1,4-dioxane being more favourable.

(2) The average thickness of the coatings is less than 0.5 and 1 nm in THF and 1,4-dioxane, respectively, suggesting patchy coatings at least from the former solvent.

(3) The dispersive and acid–base characteristics found for the PVC–PMMA blend-coated polypyrrole specimens are intermediate between those of the sorbent (polypyrrole) and the adsorbates, an indication of patchy coatings that confirms the XPS studies.

(4) Comparison of XPS and IGC results suggest that PVC–PMMA blends adsorbed onto polypyrrole from THF may form homogeneous patches. By contrast, PMMA is depleted to the free surface of the blend patches adsorbed from 1,4-dioxane. The polypyrrole–(PVC–PMMA) blend interface is thus PVC-rich at least in the case of 1,4-dioxane. This is in agreement with the conclusions drawn from TOF-SSIMS results.

Beyond this specific study of conducting polymer surfaces, it is shown that IGC is a unique tool for studying multicomponent systems with complex interfacial interactions and possible segregation of species to or depletion from the surface. However, it is also stressed that combining IGC with powerful techniques such as XPS and SIMS is of paramount importance for providing fine details on the surface chemistry and thermodynamics of materials interfaces.

Acknowledgements

M-LA, MMC and JFW wish to thank the British Council and the French Foreign Office (Ministère des Affaires Etrangères) for travel funds through the Anglo-French Alliance scheme (No. 94101) to support this research programme.

References

[1] T.J. Skotheim (Ed.), Handbook of Conducting Polymers, Vols. 1 and 2, Marcel Dekker, New York, 1986.
[2] J.L. Bredas, R. Sielby (Eds.), Conjugated Polymers: The Novel Science and Technology of Highly Conducting and Nonlinear Optically Active Materials, Kluwer, Dordrecht, 1991.
[3] P. Kathirgamanathan, in: A.H. Fawcett (Ed.), High Value Polymers, Royal Society of Chemistry, Cambridge, 1991.
[4] M. Aldissi (Ed.), Intrinsically Conducting Polymers: An Emerging Technology, Kluwer, Dordrecht, 1993.
[5] H.S. Nalwa (Ed.), Handbook of Organic Conductive Molecules and Polymers, Vols. 1–3, Wiley, Chichester, 1997.
[6] M.-A. De Paoli, in: H.S. Nalwa (Ed.), Handbook of Organic Conductive Molecules and Polymers, Vol. 2, Wiley, Chichester, 1997, p. 773, Ch. 18.
[7] F.D. Kumar, R.C. Sharma, Eur. Polym. J. 34 (1998) 1053.

[8] S.A. Xuejun, S.A. Jenekhe, Macromolecules 33 (2000) 2069.
[9] O. Ouerghi, A. Senillou, N. Jaffrezic-Renault, C. Martelet, H. Ben Ouada, S. Cosnier, J. Electroanal. Chem. 501 (2001) 62.
[10] F. Beck, R. Michaelis, J. Coat. Technol. 64 (1992) 59.
[11] W.B. Wessling, in: H.S. Nalwa (Ed.), Handbook of Organic Conductive Molecules and Polymers, Vol. 3, Wiley, Chichester, 1997, p. 497, Ch. 11.
[12] C.A. Ferreira, S. Aeiyach, J.-J. Aaron, P.-C. Lacaze, in: P.C. Lacaze (Ed.), Organic Coatings, AIP Press, London, 1995, p. 153.
[13] V.J. Jie He, V.J. Gelling, D.E. Tallman, G.P. Bierwagen, G.G. Wallace, J. Electrochem. Soc. 147 (2000) 3667.
[14] D.E. Tallman, Y. Pae, G.P. Bierwagen, Corrosion 55 (1999) 779.
[15] D.E. Tallman, Y. Pae, G.P. Bierwagen, Corrosion 56 (2000) 401.
[16] H. Naarman, Synth. Metals 41–43 (1991) 1.
[17] E. Ruckenstein, S. Wang, Polymer 34 (1993) 4655.
[18] Y.H. Lee, J.Y. Lee, D.S. Lee, Synth. Metals 114 (2000) 347.
[19] H. Chriswanto, H. Ge, G.G. Wallace, Chromatographia 37 (1993) 423.
[20] C. Perruchot, M.M. Chehimi, M. Delamar, F. Fievet, Surf. Interface Anal. 26 (1998) 689.
[21] C.L. Heisey, J.P. Wightman, E.H. Pittman, H.H. Kuhn, Textile Res. J. 63 (1993) 247.
[22] C. Forder, S.P. Armes, A.W. Simpson, C. Maggiore, M. Hawley, J. Mater. Chem. 3 (1993) 563.
[23] F. Faverolle, A.J. Attias, B. Bloch, P. Audebert, C.P. Andrieux, Chem. Mater. 10 (1998) 740.
[24] S.P. Armes, B. Vincent, J. Chem. Soc., Chem. Commun. (1987) 288
[25] S. Maeda, S.P. Armes, J. Colloid Interface Sci. 159 (1993) 257.
[26] S.F. Lascelles, G.P. McCarthy, M.D. Butterworth, S.P. Armes, Colloid Polym. Sci. 276 (1998) 893.
[27] M. Omastova, J. Pavlinec, J. Pionteck, F. Simon, S. Kosina, Polymer 39 (1998) 6559.
[28] M.A. Khan, S.P. Armes, Adv. Mater. 12 (2000) 671.
[29] M.M. Chehimi, E. Pigois-Landureau, M. Delamar, J. Chim. Phys. 89 (1992) 1173.
[30] M.M. Chehimi, M.-L. Abel, E. Pigois-Landureau, M. Delamar, Synth. Metals 60 (1993) 183.
[31] E. Pigois-Landureau, M.M. Chehimi, J. Appl. Polym. Sci. 49 (1993) 183.
[32] M.M. Chehimi, M.-L. Abel, E. Pigois-Landureau, M. Delamar, Le Vide, Les Couches Minces 268 (Suppl.) (1993) 105.
[33] M.M. Chehimi, S. Lascelles, S.P. Armes, Chromatographia 41 (1995) 671.
[34] M.M. Chehimi, in: J.-P. Caliste, E. Truyol, J. Westbrook (Eds.), Thermodynamical Modeling and Materials Data Engineering, CODATA/Springer, Berlin, 1998, p. 135.
[35] M.M. Chehimi, in: N.P. Cheremisinoff, P.N. Cheremisinoff (Eds.), Handbook of Advanced Materials Testing, Marcel Dekker, New York, 1995, Ch. 33.
[36] M.M. Chehimi, M.-L. Abel, Z. Sahraoui, K. Fraoua, S. Lascelles, S.P. Armes, Int. J. Adhesion Adhesives 17 (1997) 1.
[37] M.M. Chehimi, M.-L. Abel, C. Perruchot, M. Delamar, S.F. Lascelles, S.P. Armes, Synth. Metals 104 (1999) 51.
[38] M.M. Chehimi, M.-L. Abel, Z. Sahraoui, J. Adhesion Sci. Technol. 10 (1996) 287.
[39] C. Perruchot, M.M. Chehimi, M. Delamar, S.F. Lascelles, S.P. Armes, J. Colloid Interface Sci. 193 (1997) 190.
[40] G. Markham, T.M. Obey, B. Vincent, Colloids Surf. 51 (1990) 23930.
[41] R.A. Bailey, K.C. Persaud, Anal. Chim. Acta 363 (1998) 147.
[42] K.L. Mittal, H.R. AndersonJr. (Eds.), Acid–Base Interactions: Relevance to Adhesion Science and Technology, VSP, Utrecht, 1991.
[43] K.L. Mittal (Ed.), Acid–base Interactions: Relevance to Adhesion Science and Technology, Vol. 2, VSP, Utrecht, 2000.
[44] F.M. Fowkes, J. Adhesion Sci. Technol. 4 (1990) 669.
[45] T.B. Lloyd, Colloids Surf. A 93 (1994) 25.
[46] M.M. Chehimi, in: K.L. Mittal, A. Pizzi (Eds.), Adhesion Promotion Techniques. Technological Applications, Marcel Dekker, New York, 1999, p. 27, Ch. 2.
[47] M.-L. Abel, M.M. Chehimi .M., A.M. Brown, S.R. Leadly, J.F. Watts, J. Mater. Chem. 5 (1995) 845.
[48] M.M. Chehimi, M.-L. Abel, M. Delamar, J.F. Watts, P.A. Zhdan, in: P.C. Lacaze (Ed.), Organic Coatings, AIP Press, London, 1995, p. 351.
[49] M.M. Chehimi, M.-L. Abel, B. Saoudi, M. Delamar, N. Jammul, J.F. Watts, P.A. Zhdan, Polimery 41 (1996) 75.
[50] M.-L. Abel, M.M. Chehimi, Synth. Metals 66 (1994) 225.
[51] M.-L. Abel, J.L. Camalet, M.M. Chehimi, J.F. Watts, P.A. Zhdan, Synth. Metals 81 (1996) 23.
[52] D.J. Walsh, J.G. McKeown, Polymer 21 (1980) 1330.
[53] J.J. Schmidt, J.A. Gardella Jr., L. Salvati Jr., Macromolecules 22 (1989) 4489.
[54] D. Briggs, Spectrosc. Eur. 5 (1993) 8.
[55] S.T. Jackson, R.D. Short, J. Mater. Chem. 2 (1992) 259.
[56] D. Briggs, I.W. Fletcher, S. Reichlmaier, J.L. Agulo-Sanchez, R.D. Short, Surf. Interface Anal. 24 (1996) 259.
[57] M.-L. Abel, S. Leadley, A. Brown, J. Petitjean, M.M. Chehimi, J.F. Watts, Synth. Metals 66 (1994) 85.
[58] Z. Al-Saigh, P. Munk, Macromolecules 17 (1984) 803.
[59] J.R. Conder, C.L. Young (Eds.), Physicochemical Measurement by Gas Chromatography, Wiley, Chichester, 1979.
[60] V. Gutmann (Ed.), The Donor–Acceptor Approach to Molecular Interactions, Plenum Press, New York, 1978.
[61] F.L. Riddle Jr., F.M. Fowkes, J. Am. Chem. Soc. 112 (1990) 3259.
[62] E.F. Meyer, J. Chem. Ed. 57 (1980) 120.
[63] T.J. Carney, P. Tsakiropoulos, J.F. Watts, J.E. Castle, Int. J. Rapid Solidification 5 (1990) 189.
[64] F.M. Fowkes, M.A. Mostafa, Ind. Eng. Chem. Prod. Res. Dev. 17 (1978) 3.
[65] G.M. Dorris, D.G. Gray, J. Colloid Interface Sci. 77 (1980) 353.
[66] D.J. Brookman, D.T. Sawyer, Anal. Chem. 40 (1968) 106.
[67] C. Saint Flour, E. Papirer, Ind. Eng. Chem. Prod. Rev. 21 (1982) 666.
[68] J. Vial, A. Carré, Int. J. Adhesion Adhesives 11 (1991) 140.